Subsurface geologic, geophysical and chronological data for paleo-hydrologic reconstructions in Danube's lower floodplain - delta system

Florin Filip[1,2] and Liviu Giosan[1,3]**

[1] *Institute for Fluvial and Marine Systems, ZIP 024056, Bucharest, Romania; felipe@ifms.org.ro*

[2] *Fad Smart Technology, ZIP 024056, Bucharest, Romania; felipe_fad@yahoo.com*

[3] *Woods Hole Oceanographic Institution, Woods Hole, MA 02543, USA; lgiosan@whoi.edu*

** Correspondence: felipe_fad@yahoo.com; lgiosan@whoi.edu*

This manuscript has been submitted for publication in DATA journal (ISSN: 2306-5729). Please note that it has not been peer-reviewed and the final published manuscript may contain different content. If accepted, the final version of this manuscript will be available via the 'Peer-reviewed Publication DOI' link on the right-hand side of this webpage. Please feel free to contact any of the authors; we welcome feedback.

Subsurface geologic, geophysical and chronological data for paleo-hydrologic reconstructions in Danube's lower floodplain - delta system

Florin Filip[1,2] and Liviu Giosan[1,3]**

[1] Institute for Fluvial and Marine Systems, ZIP 024056, Bucharest, Romania; felipe@ifms.org.ro
[2] Fad Smart Technology, ZIP 024056, Bucharest, Romania; felipe_fad@yahoo.com
[3] Woods Hole Oceanographic Institution, Woods Hole, MA 02543, USA; lgiosan@whoi.edu

** Correspondence: felipe_fad@yahoo.com; lgiosan@whoi.edu*

Abstract: Records of paleofloods can be reconstructed from special fluvial sedimentary environments such as oxbows; however, deposits in in such lakes, if they exist at all, are still short, on the order of hundreds of years. Longer sedimentary records need to be developed for evaluating paleo-hydrologic regimes of large rivers transiting from a natural Holocene to Anthropocene. Here we report core logs, radiocarbon dates and electrical resistivity tomography data from the Danube lower region and delta collected toward evaluating their potential for paleohydrological reconstructions.

Data Set: See below and data.

Keywords: Danube; large rivers; deltas; paleo-floods; augering; drill cores; ERT; radiocarbon

1. Summary

World's major rivers have been strongly modified to support irrigation, commercial navigation, flood mitigation, and power generation [1]. Engineering modifications have altered water discharge and sediment load affecting the channel morphology and floods magnitude and frequency [2]. As instrumental streamflow records are too short to evaluate the range of natural hydrological variability paleo-flood reconstructions are essential to integrate in flood mitigation strategies. Although the Danube features one of the longest series of daily water discharge records since 1840, it is still not long enough to cover anthropogenic modifications since at least the Roman times or even the period extensive early engineering modifications in Central Europe [3]. Records of paleofloods can be reconstructed from special fluvial sedimentary environments such as oxbows [3]; however, deposits in in such lakes, if they exist at all, are still short, on the order of hundreds of years. Longer sedimentary records need to be developed for evaluating paleo-hydrologic regimes of Danube transiting from a natural Holocene to Anthropogenic.

Geologic data described herein (Fig. 1) consist of logs of drill core collected in September, 2007 in Sfantu Gheorghe (St. George) at the shore of Danube delta (Fig. 2), logs for manual auger collected in August, 2021 in lakes Jijila and Crapina (Fig. 3) and logs of drill core collected in March, 2022 in Insula Mare a Brailei (Great Islet of Brăila) (Fig. 4). The latter two regions are both located in the pseudo-deltaic transition zone between the lower floodplain and the proper Danube delta. Geophysical data consist of an electrical resistivity tomography (ERT) profile collected in August, 2021 on the Great Islet of Braila (Figs. 4 and 5). Chronological data reported are radiocarbon dates from Jijila Lake and Crapina Lake as well as from the drill core on the Great Islet of Braila (Table 1).

2. Data Description

The ERT raw dataset is available as .stg file format (see Supplementary Data). Core logs are presented visually in Figs. 2 through 4. Radiocarbon dates are reported in Table 1.

Data

The inversion of resistivity data is a combination of forward simulation and reverse simulation, with the final result of producing the structural model of the subsoil (5) (basement image obtained based on the resistivity data measured on the ground surface).

First, a direct simulation or modeling is performed (virtual prospecting, a model-to-date application, cause-to-effect), on a model built on the basis of aprior information, known (distribution of apparent resistivity in the basement, electrode configuration) or presumed (average resistivity of a sector, user hypothesis or basement structure), obtaining a set of synthetic data. Direct modeling (the direct solution) is obtained by solving the equation with partial derivatives in the range of the Fourier transform:

$$\frac{\partial}{\partial x}\left(\sigma\frac{\partial V}{\partial x}\right)+\frac{\partial}{\partial z}\left(\sigma\frac{\partial V}{\partial z}\right)-k^2\sigma V=-I\cdot\delta(x)\cdot\delta(z),$$

where, V - the scalar electric potential in the range of the Fourier transform,

I - is the intensity of the electric current of the source,

σ - is the electrical conductivity, a function size of (x,y), the inverse of resistivity.

The synthetic dataset (the measured apparent resistivity section) is then subjected to a reverse simulation (process of determining model parameters, a data-to-model application, effect-to-cause), in order to reconstruct the resistivity distribution in subsoil on the basis of **V** and **I** data measured on the surface. This gives a footnote model (the calculated apparent resistivity section) that is compared to the initial synthetic model and modified by successive iterations until the difference between them falls below a set threshold. The mean quadratic error (RMS Error, Rooth Mean Squared Error) characterizes the concordance between the data measured in the field and the calculated data of the model:

$$\mathrm{RMS}=\sqrt{\frac{\sum_{i=1}^{N}\left(\frac{d_i^{Pred}-d_i^{Meas}}{d_i^{Meas}}\right)^2}{N}}\times 100\%,$$

where, N - the total number of measurements,

d^{pred} - predictable data,

d^{meas}- the measured data.

The inversion of the resistivity data is therefore a process in which the model (inverted resistivity section) is constructed starting from the distribution of the apparent resistivity in the basement (pseudo section of measured apparent resistivity), resistivity determined by measuring at the ground surface the intensity of the injection current **I** and the voltage between the measuring electrodes **ΔV.**

The end result is the Inverted Resistivity Section (6), which represents the resistivity distribution in the basement reconstructed by the process of inversion of synthetic data. It is the end result of the electrical investigation, an image in direct connection with the geological structure of the subsoil from the point of view of the electrical properties of its various components. Based on this image and taking into account all the geological and any other data from the investigated perimeter, the user engages in the final process of geological interpretation of the geophysical results.

Radiocarbon dates are reported raw but could be calibrated if reservoir and hardwater effects are known or other assumptions hold (***).

3. Methods

Continuous coring drilling at St. George [Lat/Lon: 44° 54' 01.2537" N, 29° 36' 01.2790" E] was executed with a Boart Longyear drill rig using a double core barrel tube with a diameter of 110 mm with polycarbonate liner and core catcher. In layers of unconsolidated sands the recovery rate was [74%]. Lithology in these layers was reported and logged as sandy based on coring recovery and washings in the drill mud. For the advancement of the, A combination of rotary and weight pressing/hydraulic was use for drilling. Continuous coring drilling on the Great Islet of Braila Lat/Lon: 45° 12' 43.1361" N, 27° 59' 04.7238" E was executed with a Beretta drilling rig equipped with a triple core barrel tube and protective casing. Samples were collected in transparent polycarbonate liners. The phreatic level was reached at 1,5m and the lithology was dominated by unconsolidated sands; therefore, the recovery rate was 63%. We advance in first meters with pushing technique and after that with mixt technique pushing and rotary. Lakes Jijila Lat/Lon: 45° 21' 26.4734" N, 28° 06' 53.4325" E and Crapina Lat/Lon: 45° 17' 26.7666" N, 28° 22' 01.3015" E were manually augered during a drought period when lake levels were minimal and augering sites were dry. using a thin-wall Eijkelkamp auger 50 cm long and 1 inch wide. Sediments were then transferred in diamagnetic u-channels 1 inch wide.

Resistivity methods depend on the interdependence between the structure of the subsoil and its resistivity, measured at the surface. They are based on the resistivity contrast between different rocks and geological formations of a given area. Resistivity is measured in the field with an AMNB quadrupolar device consisting of an AB emission line through which a current of intensity I is introduced into the ground through 2 A, B emission electrodes and an MN reception line through which the difference in the potential ΔV created between the M, N electrodes when the current passes through the resistance represented by the subsoil is measured. Results are represented in the form of vertical resistivity sections, which show the distribution of this parameter by direction and depth, in direct correlation with the geological structure of the subsoil up to a maximum depth that depends on the spacing between the electrodes.

The geological interpretation of resistivity sections is based on the information available in the investigated area – geological, geophysical, geochemical data from the authorities and from the locals. Anomalies of minimum resistivity may reflect presence of clay or pore water in rocks. Saltwater produces the most intense minimum anomalies. A rock saturated with water can be over an order of magnitude more conductive than the same dry rock. Presence of saltwater decreases resistivity by another order of magnitude. In the case of a dipole-dipole configuration, such as the one used in our case, the depth of investigation is directly proportional to the distance between the means of the transmitting and receiving dipoles. The value of the apparent resistivity is calculated according to Ohm's Law in a homogeneous medium:

$$\rho a = K \times \Delta V / I \quad (1)$$

where K - a coefficient that depends on the geometric configuration of the electrodes:

$$K = 1/AM - 1/AN - 1/BM + 1/BN \quad (2)$$

The notion of apparent resistivity ρa refers to the fact that the resistivity value recorded at a point at the surface of the land represents a weighted average of the resistivity of all the rocks located in the space crossed by the current lines generated between the emission electrodes, a value in which the highest weight is held by the resistivity corresponding to the depth of the length of the device in question.

The ERT IB1 section was measured in the Great Islet of Braila using the dipole-dipole configuration with 56 electrodes arranged at 6 m with an AGI Super String R8 equipment. It can be seen that the first 5 m are represented on a section of low resistivity values that may be associated with silt deposits but also water saturation. Usually, in the geophysical practice of ERT the first meters on the section (equal to the distance between the electrodes) are not taken into account as it is extrapolated by the inversion software. Below a conductive horizon with resistivity values of 10 Ohm-m represented on ERT in green tints that may be associated with clay deposits with silt intercalations. The more resistive horizon between 9 and 14 m depth with values of 16 Ohm-m represented in yellow and orange may be associated with deposits of clays, well-compacted, with sand intercalations. In the depth range of 14 to 25m, the more conductive horizon represented on the ERT section by green tints and light blue may be associated with sandier deposits with clay intercalations, but probably strongly wetted possibly by an aquifer that reduces the resistivity contrasts. Under this horizon, down to ~57 m a more conductive horizon with resistivity values of 24.4 Ohm-m represented by colors of red and dark orange may indicate gravel with well-compacted clay and silty clay intercalations.

Organic (individual plant remains from peat) and inorganic carbon (mollusk remains) were dated at National Ocean Sciences Accelerator Mass Spectrometry (NOSAMS in Woods Hole, MA, USA) in cores at the St George, the Great Islet of Braila and augers in lakes Crapina and Jijila (Table 1). Dated mollusks were estimated to be *in situ* based on the lack of abrasion and secondary encrustations, non-exotic character (i.e., the lithological and facies characteristics of sediments that preserved them is in agreement with their known modern habitat), and sediment filling similar to the sediment surrounding the shells.

Acknowledgments: This survey was supported by a grant to Florin Filip from UEFISCDI PN-III-P1-1.1-PD-2019-0687 and grants from Woods Hole Oceanographic Institution to Liviu Giosan.

References

1. Meybeck, M. Global analysis of river systems: from Earth system controls to Anthropocene syndromes. Phil. Trans. R. Soc. Lond. B 358, 1935–1955 (2003)
2. Munoz, S.E., Giosan, L., Therrell, M.D., Remo, J.W., Shen, Z., Sullivan, R.M., Wiman, C., O'Donnell, M. and Donnelly, J.P., 2018. Climatic control of Mississippi River flood hazard amplified by river engineering. Nature, 556(7699), pp.95-98.
3. Giosan, L., Coolen, M.J., Kaplan, J.O., Constantinescu, S., Filip, F., Filipova-Marinova, M., Kettner, A.J. and Thom, N., 2012. Early anthropogenic transformation of the Danube-Black Sea system. Scientific Reports, 2(1), pp.1-6.
4. Ghenea, C. and Mihailescu, N., 1991. Palaeogeography of the Lower Danube Valley and the Danube Delta during the last 15 000 years. In Temperate palaeohydrology. Fluvial processes in the temperate zone during the last 15 000 years (pp. 343-364).
5. Telford WM, Geldart LP, Sherif RE (1990) Applied geophysics, 2nd edn. Cambridge University Press, Cambridge, UK
6. Dahlin T (2001) The development of DC resistivity imaging techniques. Comput Geosci 27:1019–1029

Table 1. Radiocarbon dates.

No.	Site	Depth (m)	Lab. No.	Material	14C age
1	St. George	45.50	OS-77369	*Dreissena sp.*	10600 ± 60
2	St. George	45.50	OS-65848	foliar material	9500 ± 55
3	Jijila	3.15	OS-129192	*Unio sp.*	3210 ± 20
4	Jijila	7.00	OS-130194	foliar material	4070 ± 20
5	Crapina	1.95	OS-133609	foliar material	1970 ± 20
6	Crapina	5.30	OS-133607	foliar material	4500 ± 25
7	Crapina	8.75	OS-130195	foliar material	5270 ± 20
8	Braila	8.00	OS-166329	foliar material	5,740± 25
9	Braila	17.50	OS-166334	foliar material	7,500± 35
10	Braila	24.59	OS-166335	foliar material	8,110± 35

Figure 1. The study region with drilling, augering site and ERT profile locations.

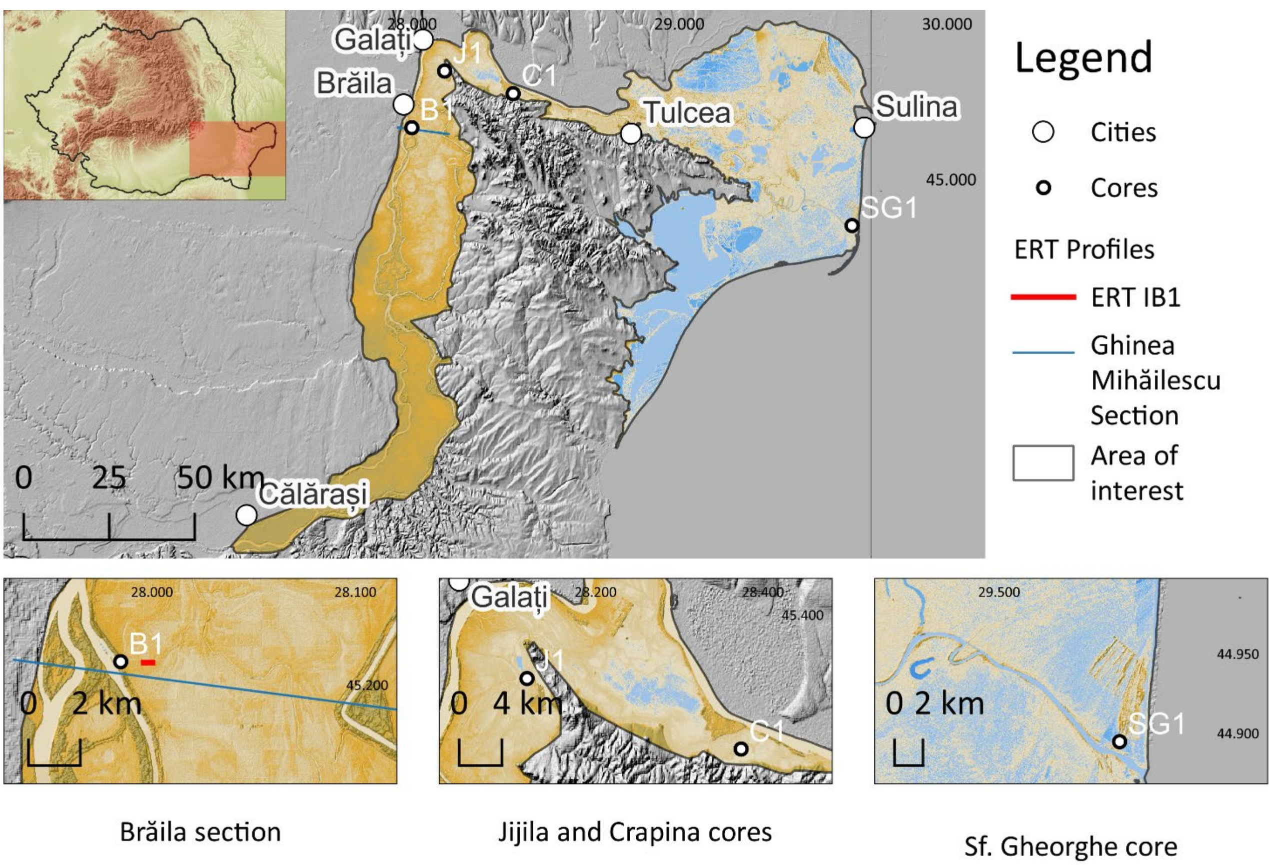

Figure 2. Sf. Gheorghe (St. George) drill core log.

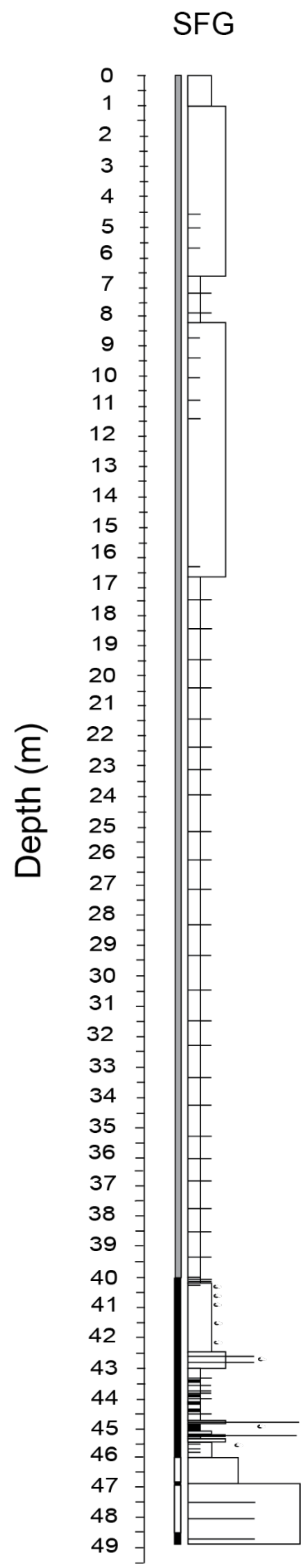

Figure 3. Logs for manual auger in lakes Jijila and Crapina.

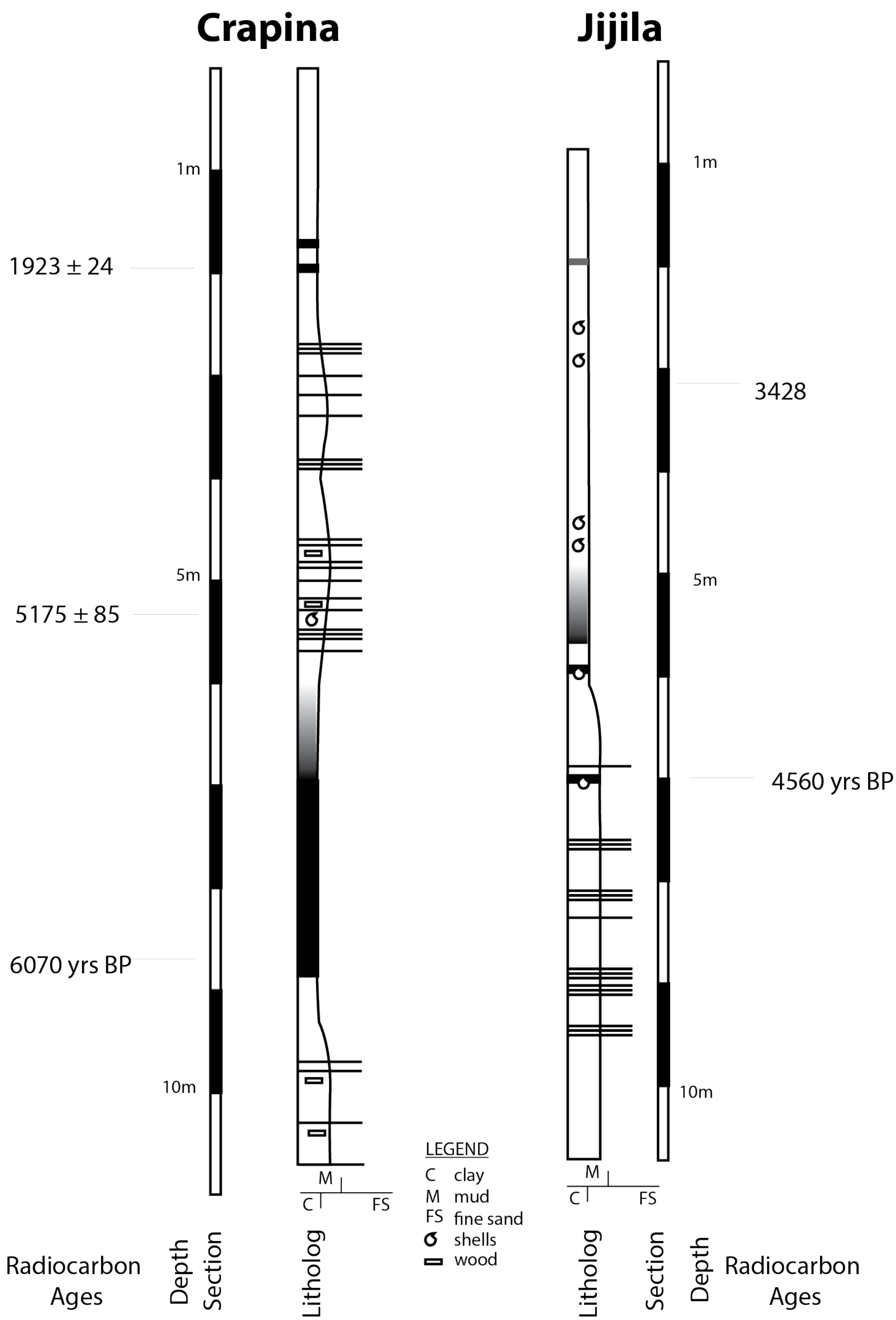

Figure 4. Drill core log from the Great Isle of Braila in the context over previous lithological information of the region [4] and our collected ERT profile.

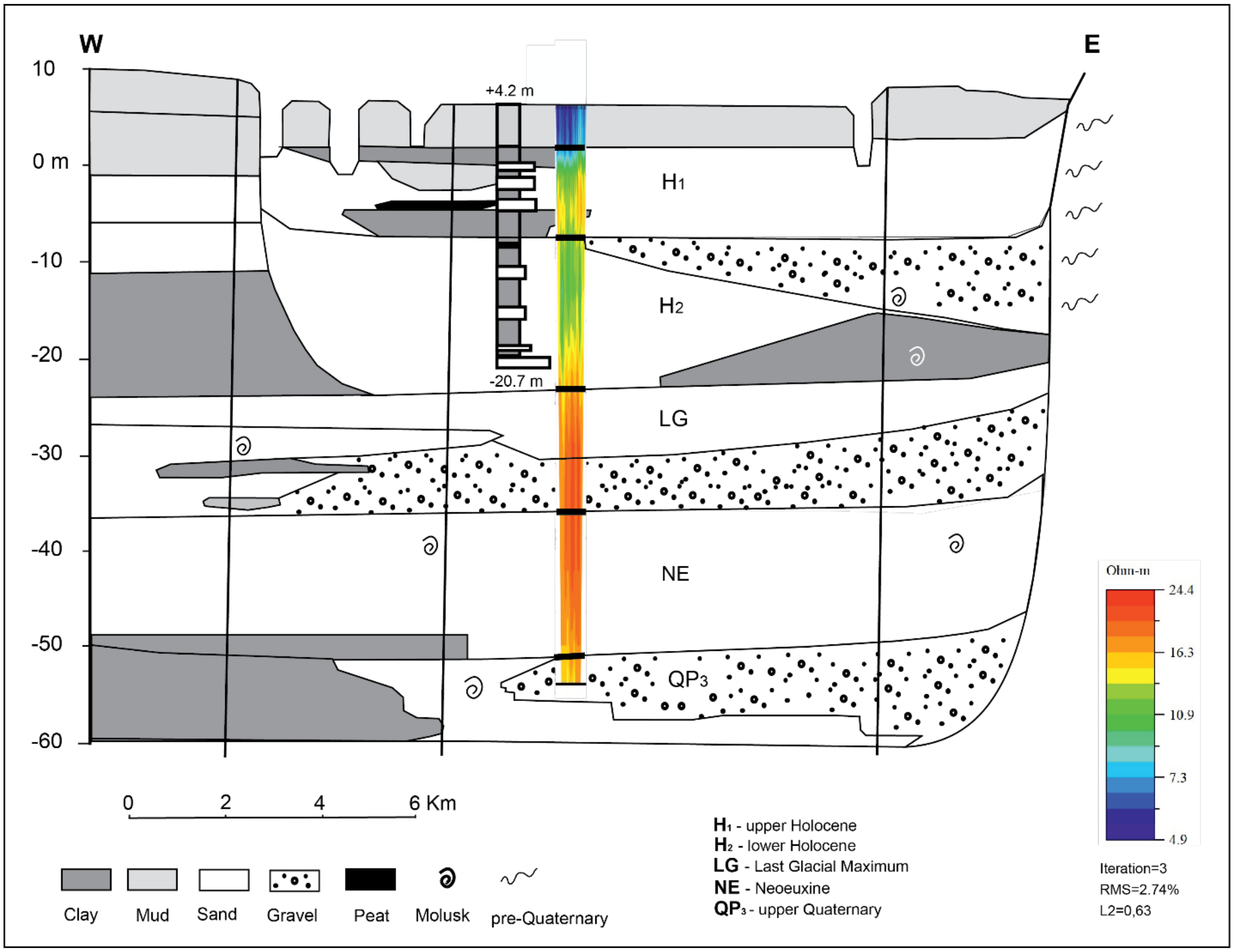

Figure 5. ERT profile on the Great Isle of Braila.